Annual westward propagating anomalies near 26°N and eddy generation south of the Canary Islands: remote sensing (altimeter/SeaWiFS) and *in situ* measurement

Robin Pingree*[†][∫] and Carlos Garcia-Soto[‡]

*Institute of Marine Studies, University of Plymouth, Drake Circus, Plymouth, PL4 8AA, UK.
[†]The Laboratory, Citadel Hill, Plymouth, PL1 2PB, UK. [‡]Centro Oceanográfico de Santander, Instituto Español de Oceanografía
(IEO), Ministerio de Ciencia y Tecnología (MCyT), Promontorio de San Martin s/n, 39004 Santander, Spain.
[∫]Corresponding author, e-mail: rdpi@mba.ac.uk

Seasonal changes in altimeter data are derived for the North Atlantic Ocean. Altimeter data are then used to examine annually propagating structure along 26°N. By averaging the altimeter data into monthly values or by Fourier analysis, a positive anomaly can be followed from 17°W to ~50°W along ~26°N. The methods give a westward travel speed of 1° of longitude a month and a half-life of one year for the average decaying structure. At ~50°W 26°N, the average structure is about 2.8 years old with an elevation signal of ~1 cm, having travelled ~3300 km westward. The mean positive anomaly results from the formation of anticyclonic eddies which are generally formed annually south of the Canary Islands by late summer and which then travel westward near 26°N. Individual eddy structure along 26°N is examined and related to *in situ* measurements and anomalies in the annual seasonal concentration cycle of SeaWiFS chlorophyll-*a*.

INTRODUCTION

In an earlier paper (Pingree, 1996), the movement and hydrographic structure of an anticyclonic eddy called *swesty* was described. The eddy was followed continuously by drogued (with drogues at 200 m depth) Argos buoys over a period of 16 months (~May 1993 to September 1994) during which time the eddy had travelled a distance of 1650 km from 25°W to 41°W near 26°N. A hydrographic survey at 33°W was conducted from RRS 'Charles Darwin' in December 1993 (PML, 1994). The core properties of temperature (19.9°C) and salinity (37.06 psu) at a depth of 190 m suggested an eddy origin near 22°W. Altimeter data indicated that positive sea level anomalies or eddy-like structure travelling westward along 26°N are more generally generated annually in summer (August), near 17°W, south of the Canary Islands. The aim of this paper is to answer the question where and when, in general, are the positive anomalies formed, what is their decay scale and how far does a positive sea level anomaly travel using altimeter data. The SeaSoar sections (~at 33°W) showed that the eddy sea surface cooling signature was only ~0.1°C and so infrared remote sensing methods (Baldacci et al., 2001) were not appropriate for this extended study. A surface SeaWiFS chlorophyll-*a* signature is evident in the Eastern Boundary region (to ~28°W) and this is shown to be caused by a redistribution of surface concentrations of chlorophyll-*a* by the swirl currents in the eddy rather than Rossby Wave structure (Cipollini, 2001).

At 33°W, the surveyed *swesty* had a surface dynamic height anomaly of 3 dyn.cm (with respect to a pressure of 1500 dbar) comparable with noise level in the processed altimeter data in this region of the North Atlantic Ocean. To resolve regular structure at large distances the data are initially both averaged into monthly anomalies and Fourier analysed to derive an annual component. The amplitude of an eddy will be about twice the amplitude derived from Fourier analysis. Repeating phase variations define a separation distance between successive positive anomalies or a wavelength for the structure.

The term *swesty-like anomaly* or *propagation* is used here for eddies or wave-like structure. It refers to a regular annually westward propagating elevation structure with a speed of −1° of longitude a month, and phased such that the position of the positive anomaly approximately matches the monthly positions of *swesty* near ~26°N.

MATERIALS AND METHODS

The remote sensing data used in this paper are from the ERS 1/2 and Topex Poseidon satellites with altimeter data covering a ~9 y period from October 1992 to October 2001 and processed according to Le Traon et al. (1998). In the methods paper of Pingree et al. (2002), the altimeter data set was separated into an annual component and a residual. The wave and eddy structure of the residual was dependent on latitude and derived for the North Atlantic Ocean from 20°N–50°N. Pingree & Sinha (2001) showed a repeating (~200 day period) mesoscale eddy structure near 33°N (*storms*) with wave-like properties: Pingree et al. (2002) found a semi-annual wave structure at 4°N with one complete wavelength across the Atlantic Ocean from West Africa to South America and this paper also describes a more regularly propagating structure travelling large distances (>~2000 km) across the ocean on an approximately fixed path. The fixed path for *swesty-like propagation* is annually westward, near ~26°N, and there are hydrographic observations (PML, 1994;
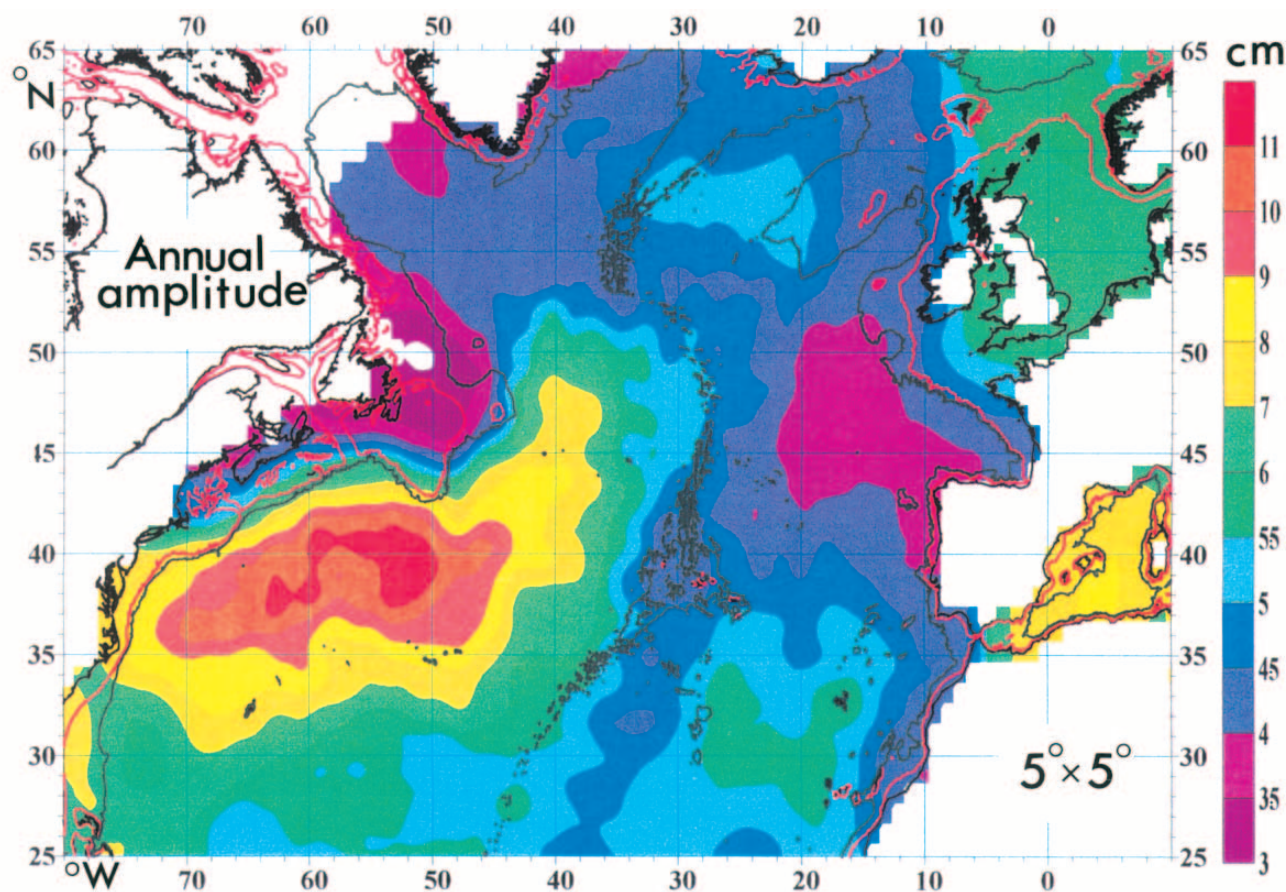
Figure 1. Annual amplitude (cm) of sea level change for the North Atlantic derived from altimeter data (using ~5°latitude× 5°longitude spatial smoothing to remove mesoscale structure) showing seasonal changes due to thermal expansion or buoyancy fluxes, wind stress and curl, and ocean circulation. The scale shows a range of 3 cm to 12 cm. The phase (not shown) is near the end of September or near the end of the heating cycle which results in a typical Eastern Basin amplitude of ~5 cm. In the Western Basin the increased amplitude in the Gulf Stream and recirculation region to the south means that the sea surface will be domed up or more anticyclonic in September–October and depressed or cyclonic in March–April.

Pingree, 1996) to relate surface elevation to the internal ocean structure. Altimeter data are examined and analysed in detail from Africa (south of the Canary Islands) to America (or the Bahama Islands). There are also *in situ* data at ~24°N (Fuglister, 1960; Roemmich & Wunsch, 1985; Lavin et al., 2003) but although the eddy or wave travels more 2000 km westward, eddy or wave influence is small at meridional distances >100 km from a mean westward track near 25.6°N. Future ocean heat flux studies are planned which will monitor ~26°N with nine profiling moorings at intervals across the Atlantic Ocean (Ocean Zone, 2003) with developments outlined in Rapidmoc (2004) and reassurance by Wunsch (2004). Longterm current meter measurements at 26°N could determine how much of an eddy's westward motion is due to advection and how much is due to phase propagation of the anticyclonic current pattern. The altimeter sea level anomalies are spatially interpolated to 0.25° in both latitude and longitude and the results presented here are relative to the mean of the total data period or are derived from Fourier analysis of amplitude and phase at a fixed position. Since the eddy signal is an annual signal, monthly mean values are derived and a Fourier perturbation method is used to separate the altimeter eddy anomaly from the seasonal or climate signal. For a ~10 y data series, monthly averaging (with each month the

~10 y average) will reduce the noise level by $\sqrt{10}$, reducing the rms value (~3 cm) to ~1 cm, so allowing regular signals to be examined well below the 2 cm accuracy goal or accuracy limit claimed for Topex Poseidon altimeter data (Cromwell & Smeed, 1998). Sea level anomalies are referred to as *sla* and monthly mean sea level anomalies are referred to as *mmsla*. Fourier analysis of the *sla* data for the annual component effectively estimates the time or phase and amplitude over the length of record. The phase of the *sla* positive maximum amplitude is referenced to the start of the year (0°). Since the annual elevation signal is mainly due to large scale heat or buoyancy storage, local annual changes in elevation due to the azimuthal geostrophic surface current structure of *swesty-like* anomalies are appraised by comparing a local signal with a larger scale annual signal. Most of the mesoscale structure due to eddies and waves in the North Atlantic (between 20°–50°N) has a spatial scale or wavelength ~13 Ro (where Ro is the Rossby radius, Ro=c/f, c is the phase speed for mode 1 internal waves and f is the coriolis parameter (see Pingree, 2002, table 3)) or ~5° of longitude, so a smoothing scale of about ~500 km will remove most of the mesoscale structure that dominates a *sla* map. A background reference or seasonal picture for the North Atlantic derived using a 5°longitude×5°latitude averaging of the *sla* data (Figure 1) is effectively without
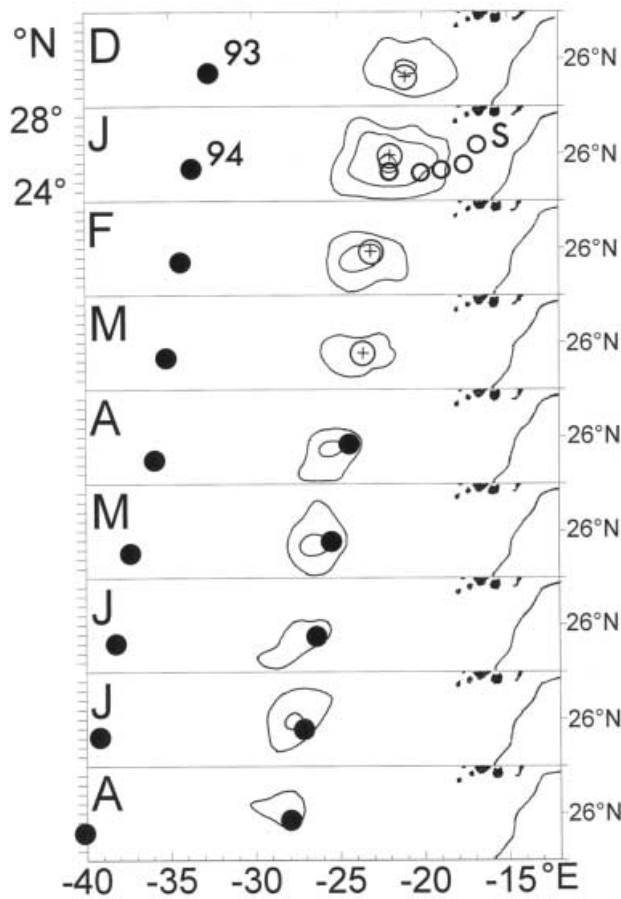
Figure 2. Contours of monthly mean sea level anomalies (*mmsla*) for zonal sections at 26°N (23.5–28.5°N, ∼555 km) for D (December) to A (August). The exterior defining contour is the first closed contour for the positive anomaly found in the region with 2 cm elevation contour intervals. The bold dot marks the position of *swesty* estimated from drogued Argos buoys tracks from mid-April 1993 to mid-August 1994. Open circles with a cross represent the monthly positions of an altimeter eddy from December 1993 (93) to March 1994. The bold open circles shown in the January (J) frame represent a positive altimeter anomaly with monthly positions shown traced back from January 2001 to September (S) 2000. Africa and the Canary Islands (blacked out) shown in the east. See text for further details.

eddy structure. In Pingree et al. (2002), it was shown that these annual variations in sea level equated with annual variations in dynamic height in the Subtropical Front region near 34°N 28°W. Near 30°N 29°W in the vicinity of the Great Meteor Tablemount, an elevation range of 14 ±2 cm between October (183 dyn.cm) and March (170 dyn.cm) was determined from conductivity–temperature–depth (CTD) data and this value can be compared with the seasonal elevation range of 11 cm in this region derived by Fourier analysis for the annual component (Figure 1), both range values larger than suggested by the analysis of Efthymiadis et al. (2002) for the CANIGO sub-region. The *in situ* studies also showed that most of the dynamic height changes occurred in the upper 500 m of the water column with opposing effects due to temperature and salinity (∼15% of temperature) changes. In shelf regions (e.g. North-western European shelf), the annual changes in sea level will have a wind set-up component (e.g. Cromwell & Smeed, 1998), and continental shelf
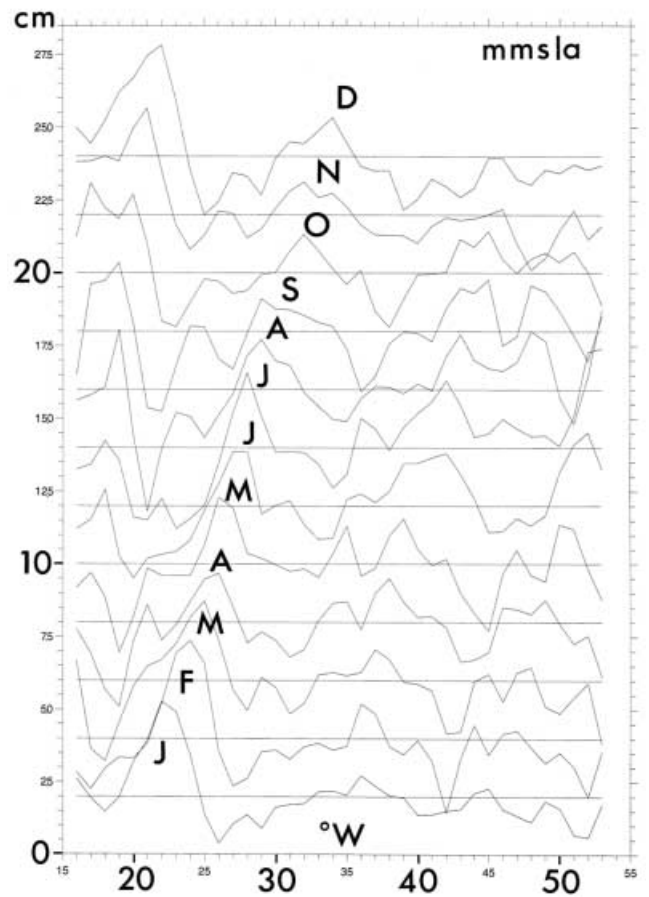

Figure 3. Monthly mean elevation structure (*mmsla*, January, J, December, D) against longitude at 25.6°N from 16°W to 53°W. Each month has its spatial mean removed (see text) and is displaced by 2 cm.
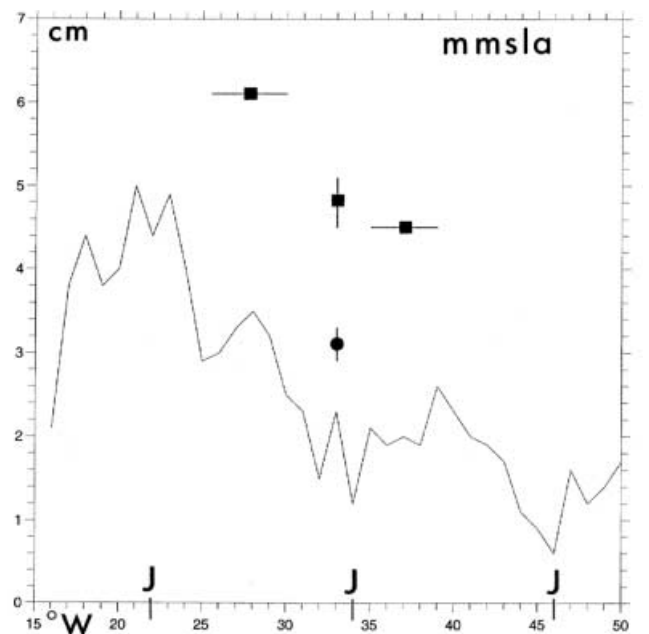

Figure 4. Amplitude of positive anomaly (cm) derived from *mmsla* against longitude (°W). Equivalent month indicated for mid-January (J). Dot with error bar near 33°W is the elevation anomaly based on dynamic height from CTD data. Also shown (squares) are the pressure head values (cm) at the centre of the eddy at a depth of 200 m derived from Lagrangian data (see text for details).
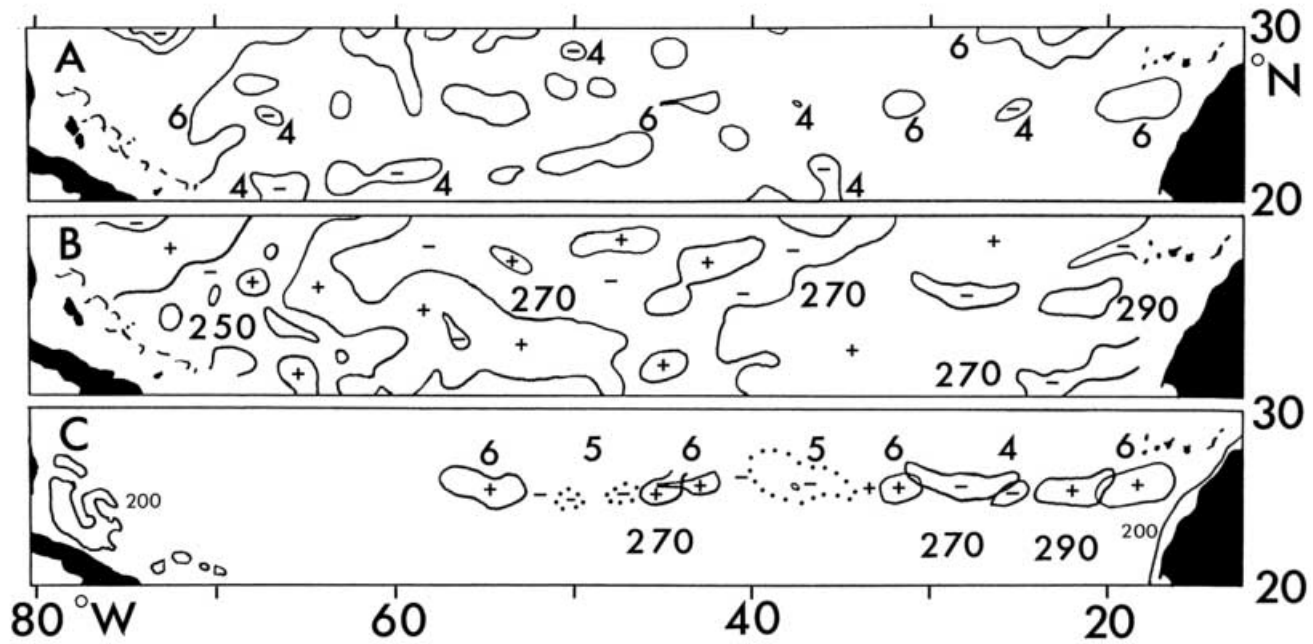
Figure 5. Contoured sections from 20°–30°N across the North Atlantic of (A) annual amplitude (cm, contour values 4 and 6 cm, below 4 cm marked with −, other closed contour have values >6 cm) and (B) phase (°, 270° is the main contour, >270° marked with + and less with −; closed 290° contour in the east and closed contours with phase <250° in the west indicated). Africa, Canary Islands, Florida, Cuba and Bahamas blanked out. In (C) maxima (with +) and minima (with −) closed contours of amplitude (cm, contour value marked above) and phase (°, contour value marked below) (from (A) and (B)) are shown between ∼25°–26°N. Additional 5 cm contour shown dotted; positions of other phase maxima and minima not evident with contour levels in (B) indicated with + and −.

poleward currents will show seasonality where elevation gradients occur near the ocean margins (Pingree et al., 1999).

The methods are used to determine the generation region, propagation speed and decay scale for the mean
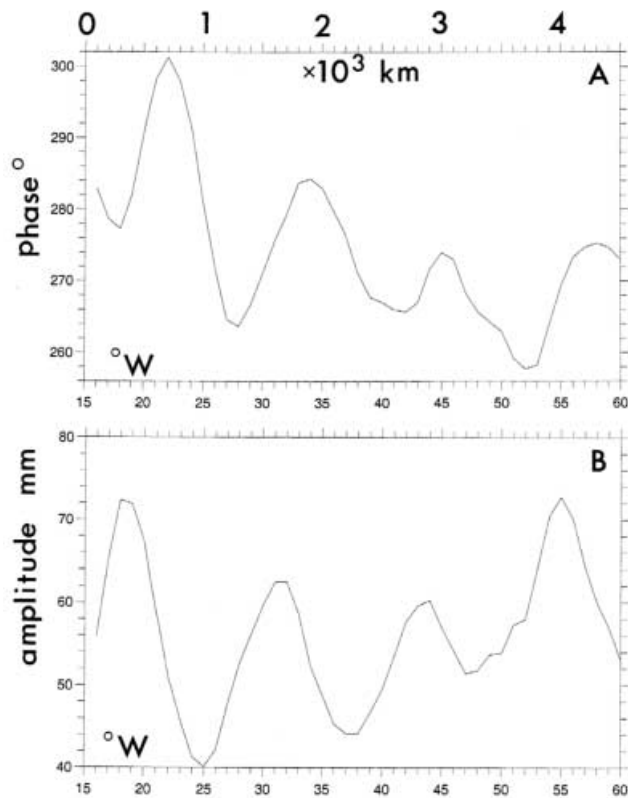

Figure 6. (A) Phase (degrees) and (B) amplitude (mm) of the annual sea surface height altimeter signal along 25.6°N against westward distance (in 10^3 km) with values from 16°W (south of the Canary Islands, between Tenerife and Gran Canaria).
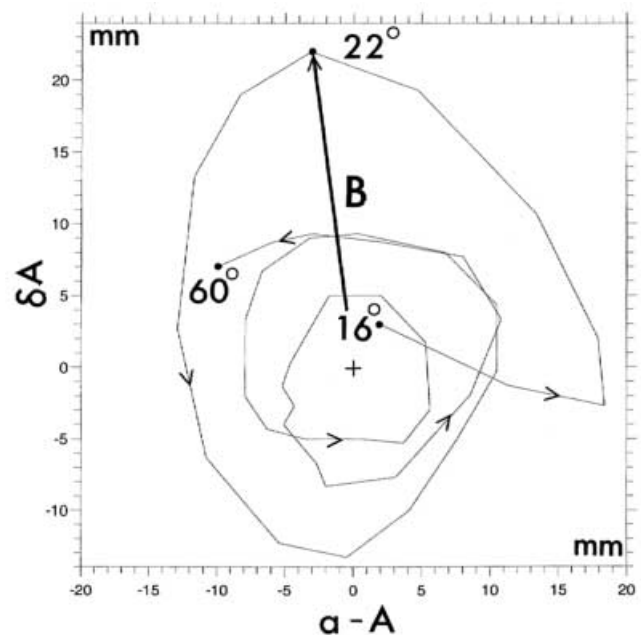

Figure 7. Phase anomaly (δA) against amplitude anomaly (a−A) in mm showing amplitude of structure, B(x), from 16°W to 60°W. Origin for B is at + (0,0) and maximum value of B=2.1 cm at 22°W shown as arrow from the origin (+).
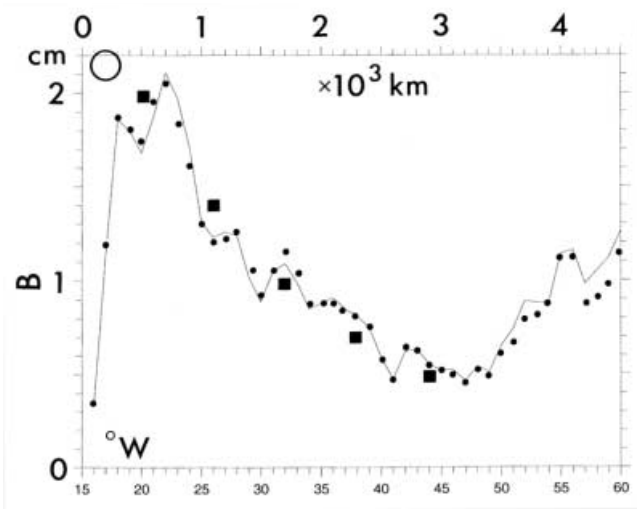
Figure 8. B (cm), or Fourier amplitude of *swesty*-like structure, against westward distance (in 10^3 km) from 16°W 60°W at 25.6°N (continuous line; dots show amplitude of structure calculated using the full expression for B, see text). Solid squares show amplitude of structure that decays to half values in one year at 600 km spacing starting with a value of 2 cm at 20°W. Open circle shows maximum value on the 17°W meridian.

annual positive anomaly travelling westward along 26°N over a ∼3300 km travel path. These values are compared with the properties of *swesty* derived from *in situ* measurement along 26°N and the distribution of individual altimeter eddies or positive anomalies near the generating region south of the Canary Islands where the altimeter signal is well resolved. A value of the positive anomaly for *swesty* was derived from CTD dynamic height data (at 33°W) and three values were calculated from the *in situ* measurements of radial current structure (see Pingree, 1996) for a depth of 200 m from Lagrangian data using the geostrophic relation. To develop further, a
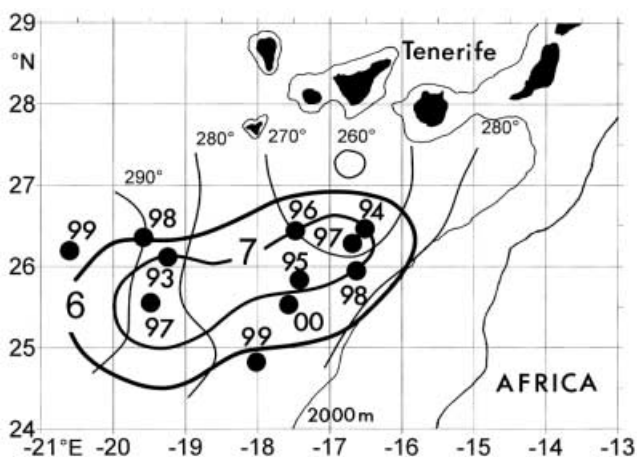

Figure 9. Summary diagram of eddy generation south of the Canary Islands (1993–2000). Bold dots represent positive sea level anomalies or eddy centres for mid-October (year given). Two eddies were generated in 1997 (97), 1998 and 1999 (see also Figure 10). Also shown are contours of amplitude (cm) and phase of the annual Fourier component (see also Figure 5) and the distributions of maximum amplitude and minimum phase contours point to an eddy origin south of Tenerife, with maximum development near 17°W 26°N by September. Canary Islands blacked out; 2000 m depth contour shown.

mean annual component (Figure 1) was subtracted from the altimeter data to resolve and examine positive elevation anomalies propagating along 26°N in individual years (1992–2002). The results are compared with *in situ* measurement and SeaWiFS chlorophyll-*a* concentration data (1997–2002) in the overlapping time window. Longitude is always referred to in °W in the text, but is given in both °W and °E in the Figures.

RESULTS

Monthly mean structure

The monthly mean sea level anomalies (*mmsla*) for the region of interest near 26°N identify the position of a closed positive elevation anomaly contour (or sea surface bump on a seasonally changing level) of initial mean scale (diameter) ∼400 km moving westward at ∼1° of longitude a month (Figure 2). The central positions derived from the monthly altimeter data match (to ∼1° of longitude, ∼1/12 the wavelength of the repeating structure) the monthly positions of the centre of the eddy *swesty*, estimated from Lagrangian data, which was also observed to move westward at ∼1° of longitude a month (from 25°W to 41°W) near 26°N. The amplitude of the structure along ∼26°N has to be determined relative to a seasonally changing background which varies between ∼+5.5 cm (September/October) and −5.5 cm (March/April), a range of ∼11 cm (Figure 1). The amplitude of the monthly anomalies along 25.6°N were derived by subtracting a mean seasonal elevation for each month, based on a mean of level from 20°W to 50°W (at 26°N). The results (Figure 3) reveal a dominant decaying positive westward propagating anomaly that forms annually. The wavelength of the repeating structure is ∼12° of longitude or ∼1200 km. Positive anomalies were estimated over a scale of ∼1000 km (with ∼3° longitude smoothing [averaging] of the *mmsla* data). The results plotted by month or longitude (Figure 4) show that the maximum mean anomaly is ∼4.5 cm near 21°W in ∼December and that this anomaly decays to half its height in ∼1 y or after 1200 km of westward travel. Values halve again to ∼1 cm at ∼45°W after a further ∼1200 km of travel. Also plotted (Figure 4) are values of pressure head (in cm) at 200 m from Lagrangian data when the eddy centre was near 27.75°W, 33°W and 37°W over a ∼9 month travel period and the sea elevation derived from CTD data (∼3 cm, based on dynamic height differences, with a reference pressure of 1500 dbar) in December 1993. The error bars for the Lagrangian data relate to the uncertainty in establishing the exterior limits of the eddy and the time taken to establish the radial current structure. For the dynamic height data, the bar is a measure of the uncertainty in the averaged difference in CTD dynamic height from CTDs near the eddy centre with respect to CTD stations at exterior positions. The pressure or elevation anomaly at the sea surface (∼3 cm) is smaller than the pressure anomaly derived at 200 m depth since the seasonal thermocline is domed upwards over the eddy core and the geostrophic surface currents correspondingly reduced. Accoustic Doppler colour profiler (ADCP) data, CTD data and SeaSoar data (Pingree, 1996) all showed that there was ∼30% reduction of currents or dynamic height
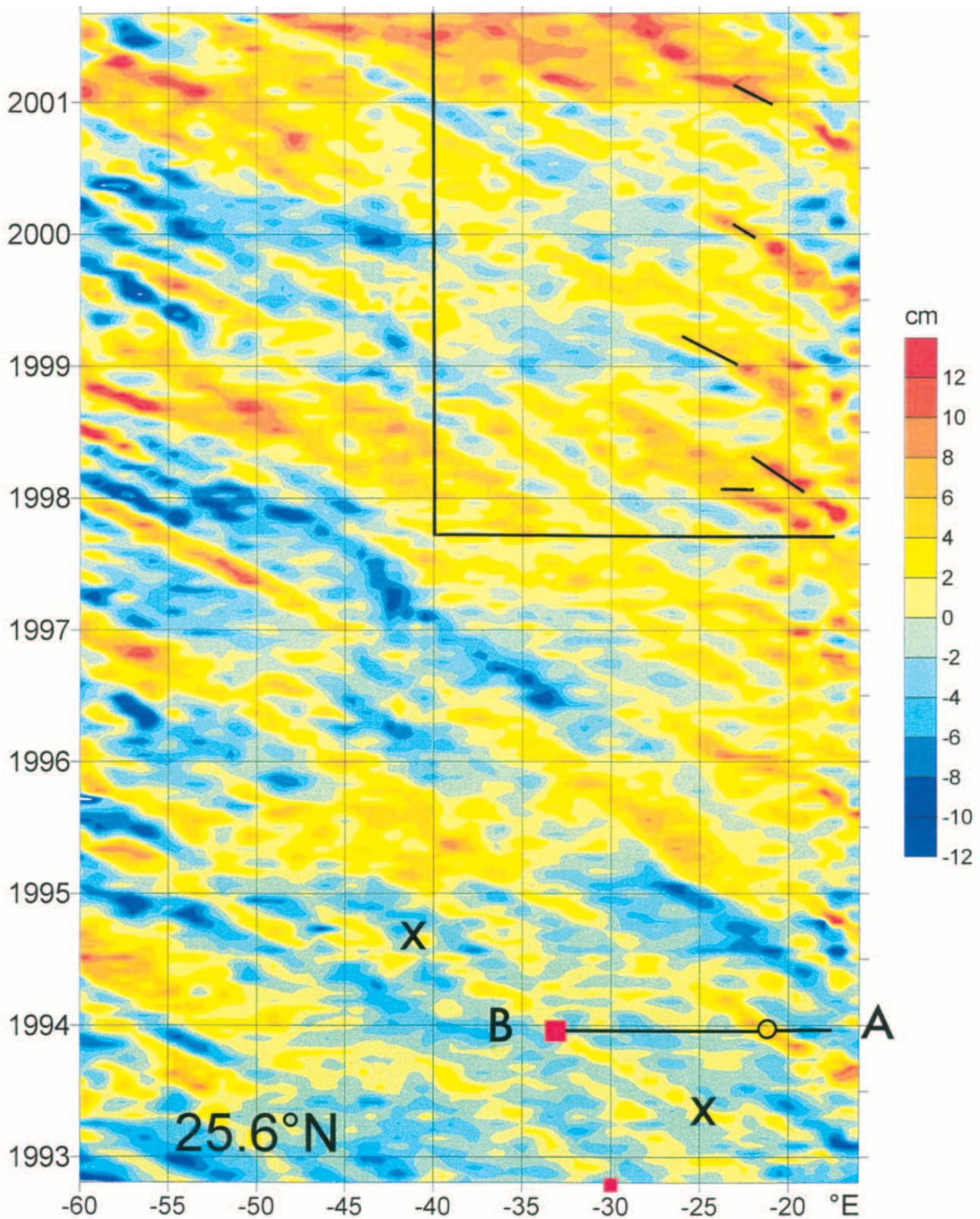
Figure 10. Hovmöller or travel contours for *swesty-like* anomalies along a path from 18° W to 60°W at 25.6°N after removing a mean annual signal to reveal more clearly the *B-like* anomalies (Figure 7). East of 18° W, the path followed is south from 27.5°N to 26.0°N along 17°W (see Figure 9). *Swesty* was followed continuously from ∼25°W to ∼41° W (marked by 'x') by Argos buoys. The line 'A' to 'B' shows the track of RRS 'Charles Darwin' along ∼26°N to the eddy survey region (red square). Open circle at ∼21° W marks the sea level anomaly about 12° to the east of *swesty*. Surface chlorophyll-*a* along A–B is shown in Figure 11. The red cross near 30°W indicates the October survey position of an open tracer release experiment. The window (top right) shows the overlap of altimeter and SeaWiFS data used in this study (see Figure 12).

Figure 12. Longitude time plot showing seasonal cycle of SeaWiFS chlorophyll *a* concentrations (mg m^{-3}) at 25.6°N over a 5 year period (1997–2002). The bloom anomaly near 23°W is associated with the westward passage of the altimeter anomaly which on average (see Figures 3 & 4) is near 23°W during the spring bloom period, early February. Anomalies or westward moving structures in the seasonal cycle are shown with red lines. These same lines are plotted in the window of Figure 10 and correspond with annually occurring westward propagating positive elevation anomalies.

Figure 11. Mid-December surface (4 m) chlorophyll-*a* (mgm^{-3}) levels at $\sim 26°$N from 16.5°W to $\sim 34°$W along the track of RRS 'Charles Darwin' in December 1993. Surface levels near the eddy (*swesty*) centre at $\sim 33°$W were ~ 0.03 mgm^{-3}. Over the eddy core, where the thermocline was do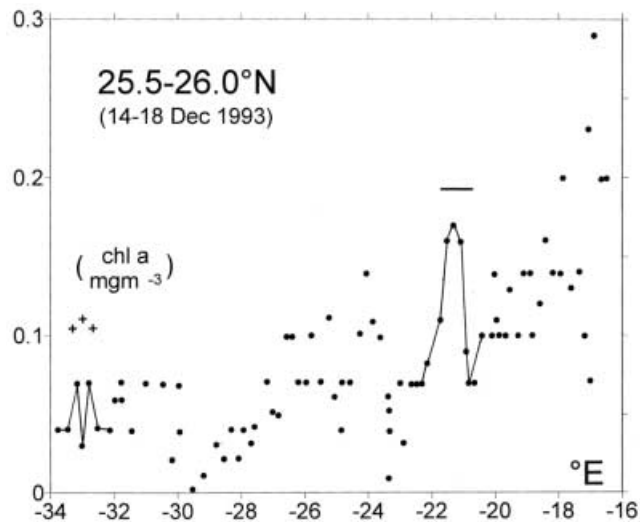med upwards (in the depth range ~ 80–120 m depth), SeaSoar sections showed the subsurface chlorophyll-*a* level was enhanced to $\sim > 0.1$ mgm^{-3} (indicated by +) locally. Increased surface levels were found between 21°–22°W where the next westward propagating sea surface elevation anomaly was crossed (position indicated by line above the maximum, also as a circle in Figure 10). Surface values increased towards the African shelf region which is influenced by enhanced levels (>1 mgm^{-3}) to the south, near 20°N, associated with West African Upwelling off Cap Blanc.

differences (equivalent to ~ 1.5 cm drop, showing that the Lagrangian datum with a value of 4.8 cm is consistent with the CTD value of 3.1 cm, within the error bars indicated) towards the sea surface with respect to a depth of 175 m. The mean rate of decay of the current structure at a depth of 200 m is $\sim 40\%$ y^{-1}, comparable with the altimeter data estimate. The surface elevation value of 3 cm compares favourably with the mean altimeter values near 33°W (and should also be compared with the actual altimeter anomaly for December 1993, see later, at 'B' in Figure 10). The Lagrangian results suggest that a postive anomaly may have an elevation of ~ 10 cm at $\sim 20°$W.

SeaSoar sections conducted during the hydrographic survey showed that a maximum displacement of isotherms (isopycnals) of ~ 70 m occurred below the eddy centre at ~ 250 m depth. The inverted magnification of internal ocean structure at ~ 250 m depth for this region (26°N 33°W) is then about $\times 2300$, considerably larger than that found for regular *Storms* at 32.5°N (Mouriño et al., 2002; Pingree et al., 2002). Thus the mean altimeter anomaly, at say the +2 cm level, although small, reflects a downward displacement of isotherms (18–19°C) of nearly 50 m at ~ 250 m depth, near 30°W.

Fourier analysis structure

One source of error in the monthly mean method that manifests itself in the scatter of adjacent positive anomaly estimates (Figure 4) occurs in establishing a reference level exterior to the anomaly. The Fourier analysis method is independent of the elevation at adjacent points or across

the positive anomaly. Fourier analysis for the annual component for a 10° latitude section (20°N–30°N) across the Atlantic Ocean, from the Canary Islands and West Africa in the east to Florida, Cuba and the Bahamas in the west, shows perturbations on a more gradually varying seasonal structure (Figure 5). By selection of contour, it can be seen that there is wavelike structure in the amplitude and phase changes in the region 24°N–27°N (Figure 5C). This can be understood by noting that in regions where the westward propagating *swesty-like* anomaly coincides with the seasonal maximum elevation (end of September or early October), then the amplitude of the annual component will be increased. In late March and early April, when the *swesty* positive anomaly has moved westward 6° of longitude, the amplitude of the annual component will show a reduced amplitude or a negative perturbation at this position. Similarly, the phase of the annual signal will show positive and negative perturbations between consecutive positive amplitude structures. Overall, there will be a regular sequence to the perturbation structure (maximum amplitude, maximum phase, minimum amplitude, minimum phase, Figure 5C) which repeats with the wavelength or distance the positive anomaly travels in one year. The shapes of the minimum and maximum contours show that the annual Fourier component is compressed meridionally with respect to the zonal direction, or in the east–west sense, with wave-like structure confined within a wave or eddy guide near 25.6°N. The amplitude and phase of the annual component along $\sim 25.6°$N shows a decaying perturbation signal for about 3500 km westward to $\sim 50°$W (Figure 6). We could take the envelope of amplitude and phase and plot the decay scales separately but it is easy to show that the amplitude and phase results can be combined for a single plot that includes all the remote sensing data, rather than just the extreme values.

For illustrative purposes, consider the combination of an annual signal, $A(x)\cos(\omega t + \phi_x)$, where $A(x)$ and ϕ_x are slowly varying functions of position, x (east) and $\omega = 2\pi/T$, where T is the annual period, and a small positive sinusoidal perturbation of range $2B(x)$, with a wavelength L (wavenumber, $k = 2\pi/L$) which propagates with phase speed $c = L/T$. Approximating A and ϕ_x with their mean values over one or more wavelength and taking a time origin, $t = 0$ at $x = 0$, when both oscillations are in phase (e.g. end of September/beginning of October near 18°W, 26°N) then the combined sea level variation, or *sla*, is given as

$$sla = A\cos(\omega t) + B(x)\cos(kx - \omega t) \qquad (1)$$

The amplitude, a, and phase anomaly, δ, of the resulting annual signal are given simply

$$a^2 = A^2 + B^2 + 2AB\cos kx \quad \text{and} \quad \tan\delta = B\sin kx/(A + B\cos kx)$$

For small B/A, and expanding to first order gives $B\cos kx = a - A$ and $B\sin kx = \delta A$. The neglect of higher order terms is not serious in this context with B/A ~ 0.2 (Figure 6), and results in a small modulation to the approximation. With k negative the perturbation travels westward. Accordingly, the perturbation amplitude anomaly, $a - A$, and the phase anomaly, δA, are derived from Figure 6 to give the two orthogonal components of B(x).

By drawing smooth envelopes to the curves (Figure 6) a mean amplitude and phase is determined at each longitude position. These essentially spatially averaged mean values are then subtracted from the annual amplitude and phase value determined by Fourier analysis at each longitude position. The phase anomaly is converted to radians and multiplied by A at each point. The resulting δA values are plotted against the amplitude anomaly (a-A) values to give the amplitude of B at successive longitudes (Figure 7). The structure for B(x) is conveniently viewed in time or distance if at each longitude the amplitude and phase components for B are squared, added and square rooted (Figure 8). We could have just taken the range of amplitudes shown in Figure 6A. For example, at 25°W a range of ~2.6 cm gives a perturbation amplitude of ~1.3 cm based on the results of Figure 6. In Figure 8, the estimate for B at 25°W is also seen to be ~1.3 cm. However, the method adopted makes use of the amplitude and phase of the annual Fourier component at each longitude, which is itself based on a record length of ~9 y. The results (Figure 8) give values of ~4 cm for the mean elevation anomaly of a *swesty*-like structure near ~20°W which fall to a half value of ~2 cm at ~32°W. The values are again half ~1 cm at about 44°W giving a decay scale of ~1200 km or a half-life of one year in a 1200 km westward travel distance over a distance of ~3000 km or a travel time of ~2.5 y, values comparable with those obtained by the monthly mean method (Figure 4), which also makes use of all the data points.

Case studies of individual eddies

In addition to matching the travel properties of the surveyed eddy with the averaged altimeter structure (see, for example, Figure 2) it is necessary to match individual positive anomaly altimeter structures with the averaged (monthly mean or Fourier) structure for a complete interpretation of structure. This is conveniently done to the east of 25°W where the altimeter positive anomaly is well resolved. From December 1993 to March 1994, the altimeter data showed a significant (~10 cm with respect to background) positive anomaly or anticyclonic eddy about 12 degrees to the east of the position of *swesty* (shown by open circle with cross in Figure 2) and the centre of the altimeter eddy was located within the defining contours of the mean structure. This is consistent with interpreting the mean structure as an ensemble average of mesoscale eddies rather than a large (400 km) eddy or wave of reduced (due to averaging) amplitude. The position of a conspicuous positive anomaly in January 2001 (Figure 2, January frame, bold open circles) can be traced back to its generating region south of Tenerife in August 2000. In like manner, the Fourier amplitude and phase distributions also reflect the positions and strength of individual eddies. For example, in October, regular annually propagating eddy structure will result in a locally increased amplitude for the annual component (see Figure 5C). The positions of all the marked anticyclonic eddies for October are superposed on the amplitude and phase structure of the annual Fourier component in Figure 9 where it is evident that the distribution of eddy centres matches the maximum amplitude contour region. The phase lines of the annual signal show that the growing perturbation of

averaged eddy amplitude propagates south-westwards from a position south of Tenerife. The anticyclonic structure is attributed to surface water flowing southward between Tenerife and Gran Canaria that adjusts anticyclonically as a surface layer thickens and so also deepens locally. Individual structure is, as is to be expected, more variable. In some years, eddy production may occur further west, between Gomera and Hiero, for example, and occasionally to the west of the Canary Islands. The characteristic temperature and salinity core properties of *Swesty* suggested an origin near 22°W in January 1993 (Pingree, 1996) and the altimeter data showed a conspicuous anticyclonic eddy near 20°W (27°N) in December 1992. In some years two eddies form (1997, 1998 and 1999, for example) and these may co-exist thus broadening the average distributions (see Figures 2 & 9). The *swesty*-like structure at 21°W (Figure 2D) was complete by August 1993 with centre near 17°W 26°N (see Tejara et al., 2002) for I.R. Signature near 26°N.

The increasing amplitude near 18°W in October (Figure 8, see also Figure 4) is to be interpreted as the arrival of structure at the 25.6°N latitude, rather than a generating region to the east. Backtracking eastwards along 25.6°N and then deviating to the north-east near 19° towards Gran Canaria (see Figure 9) gives a maximum amplitude near 17°W 26°N with maximum development by September for the mean structure and this amplitude value is plotted in Figure 8 (as a circle, equivalent to a positive anomaly of 4.3 cm). We might also expect individual structures to have a longer decay scale than that derived for the mean structure as individual eddies may spread north and south from the mean latitude at 25.6°N. Some later decay might reflect the developing seasonal thermocline isolating the eddy core and reducing surface currents. The mean positive anomaly of individual eddies near 18°W (for October) was ~13 cm.

DISCUSSION AND SUMMARY

On the oceanic scale, the results presented (Figure 1) show that large scale anomalies in the annual signal in the North Atlantic (>20°N) represent a seasonal geostrophic surface circulation that is in phase (e.g. anticyclonic autumn structure) with the heat storage cycle (together with a fresh water evaporation flux and a wind stress forcing contribution to the seasonal elevation cycle). Similarly, we should interpret those regions in the Atlantic where the annual amplitude falls to zero or is at a minimum (e.g. 10°–15°N, 20°–40°W, US WOCE, 2001; Pingree et al., 2002) as regions where the seasonal surface circulation destructively combines with the annual elevation produced by the seasonal climate cycle. From the Canary Islands to the Bay of Biscay, the seasonal amplitude decreases poleward on the ocean margin. This would tend to drive a shallow water depth seasonal poleward current which might extend to the shelf break/slope region if the density gradient anomaly persisted at depth. The maximum forcing would be in October which is also the time of maximum seasonal southward surface flow in the Canary Current, east of Madeira to the Canary Islands (from Figure 1). Further north, in the West European Shelf region, the amplitude contours align with the continental slope. Maximum elevation gradients in

this region (i.e. taking account of annual phase) indicate a maximum seasonal geostrophic poleward flow in January (see for example, Pingree et al., 1999). Major meridional components of seasonal flow in the Ocean occur near $\sim 45°$–$50°$N with maximum poleward flow in a central region in March and associated net transfer of heat poleward. Rapid circulation/climate changes as apposed to seasonal changes at $26°$N can be appraised from Figure 10 where, for example, a general central low at $30°$–$45°$W in 1996 indicates a cyclonic component or a weakening Subtropical Gyre (Pingree, 2002).

The analysis of altimeter data along $\sim 26°$N was guided by the results from measurement at sea. A hydrographic survey of an eddy (*swesty*) at $26°$N $33°$W was conducted in December 1993. Lagrangian buoy data showed that *swesty* tracked westward at a speed of $\sim 100\,\mathrm{km\,month^{-1}}$ over a distance of about $1600\,\mathrm{km}$ from $\sim 25°$W to $41°$W along $\sim 26°$N over a period of 16 months. The altimeter monthly mean and Fourier analysis results show that on average positive anomalies form annually south of the Canary Islands and travel westward at $1°$ of longitude a month near $\sim 26°$N. The altimeter data extended *swesty-like propagation* from $17°$W to $\sim 50°$W where the mean positive anomaly was $1\,\mathrm{cm}$, giving a total westward track of $\sim 3300\,\mathrm{km}$ (Figure 6). The half-life or decay scale derived from the altimeter data over the mean track (Figure 8) was ~ 1 year. At $50°$W, a positive anomaly would be nearly $3\,\mathrm{y}$ old. Backtracking and deviating from the $25.6°$N latitude near $18°$W, gives a mean generation region south of Tenerife with maximum development near $17°$W $26°$N by September. The monthly mean method and the Fourier analysis show that at any given time up to three resolved positive anomalies (separated by $\sim 1200\,\mathrm{km}$) may be found on the latitude line near $26°$N (from $17°$W–$50°$W).

The wider perspectives of decay scale studies relate to mixing and diffusion processes in the ocean. The $1/e$ decay time scale is $\tau \sim 1.5\,\mathrm{y}$ (or $\sim 1700\,\mathrm{km}$ for equivalent length scale). It is easy to show that for an oscillating structure of wavenumber, k, $(L = 2\pi/k,\ k^{-1} \sim 200\,\mathrm{km})$ with length decay scale much larger than k^{-1}, subject to horizontal diffusion, K_x, in the direction of propagation only, then $K_x = 1/(k^2\tau)$, or of order $\sim 10^3\,\mathrm{m^2\,s^{-1}}$ in this idealized context. It was noted that west of $50°$W, the annual structure increases in amplitude (Figure 8). This is believed to be due to constructive superposition of annual structures originating in the Western Basin, perhaps from the Mid Atlantic Ridge. The transect along $25.6°$N (Figure 6) was continued west to the Bahamas (Figure 5) where it intersects the Tongue of the Ocean (German et al., 2002). Although a dominant annual wavelike structure of similar amplitude was found that matched the phase at $\sim 60°$W, the wavelength of the structure west of $60°$W was $\sim 900\,\mathrm{km}$. Further studies with *in situ* data would be required to resolve the nature, origin and complexity of structures found west of $\sim 60°$W. The Fourier results also showed a north-westward propagating mesoscale annual signal with a wavelength or separation of positive anomalies of $\sim 400\,\mathrm{km}$ passing through the 1973 MODE region centred near $28°$N $70°$W (Ocean Circulation, 2001). The β-triangle survey region (Armi & Stommel, 1983), centred at $27°$N $32.5°$W, will generally (80% probability) contain a swesty centre.

The individual structures or eddies propagating west-south-west from the Canary Islands and then along $25.6°$N are conveniently displayed in the Hovmöller diagram for the sea level anomaly data (i.e. without monthly averaging) but with a mean annual component removed (Figure 10). In this case, the mean annual component is not the local value but rather a spatial mean along the travel route, $\sim 5.5\,\mathrm{cm}$ amplitude and $\sim 270°$ phase (see Figure 6). Figure 10 shows structures other than annual which were largely averaged out in the monthly mean and the Fourier analyses (Figures 4 & 8) but some semi-annual structure was evident in Figure 3. Figure 10 also shows variability in the timing of structure in the generating region near $17°$W with two positive anomalies generated in some years. The important feature for interpretation of the altimeter data signals is the positive anomaly (~ 2–$4\,\mathrm{cm}$ elevated) marked XBX (Figure 10). This is the $\sim 1600\,\mathrm{km}$ track of *swesty* from $\sim 25°$W to $\sim 41°$W as observed by Argos buoys with CTD and SeaSoar survey at B ($\sim 33°$W, in late December 1993). The positive anomalies tracking westward the year before and the year after the *swesty* XBX measurement line are evident. The red cross on the positive anomaly line the year before represents the position and time for the second survey of an open-ocean tracer-release experiment (Ledwell et al., 1993) in October 1992. The tracer was released near $25.7°$N $28.25°$W in May 1992, and in May the positive anomaly or eddy is likely to have been near $25°$W or behind the patch. The current structure of the eddy will mix the ocean as the eddy passes through. The October survey showed that the initial tracer patch ($\sim 40\,\mathrm{km}$ in May) had stretched to a curved streak $\sim 200\,\mathrm{km}$ in length between $29°$ and $31°$W. It is plausible that the tracer patch had been or was being strained by the westward passage of a *swesty-like* annual anomaly. The vertical eddy diffusivity, K_z, determined for conditions at $\sim 26°$N was $K_z = 0.15\,\mathrm{cm^2\,s^{-1}}$. For the *swesty* core, the horizontal diffusivity was determined as $K_h \sim 4\,\mathrm{m^2\,s^{-1}}$; the subduction rate was $40\,\mathrm{m\,y^{-1}}$.

The line AB is the track of RRS 'Charles Darwin' steaming westward and this intersects the positive anomaly line generated the year after the *swesty* line (see also Figure 2, December frame) near $21°$W. The surface properties (mixed to $\sim 100\,\mathrm{m}$, using XBTs) were 37.0 psu and $21.2°$C, marginally fresher (0.1 psu) and cooler ($0.2°$C) than the surrounding water. The surface salinity is expected to increase and the temperature decrease until an insulating seasonal thermocline is established about April. Eddy core characteristics are more conserved when insulated by a seasonal thermocline than during the winter mixing period of thermocline erosion. If an eddy is formed during or at the end of the winter mixing period then the eddy origin can be traced back to the region where the core characteristics occur at the sea surface. However, the positive elevation altimeter anomaly at $21°$W could be traced back to an August formation south of Tenerife near $26.5°$N (e.g. Figure 9) and here (in December 1993), the salinity was ~ 36.8 psu. The ADCP structure showed south and then north surface currents ($\sim 10\,\mathrm{cm\,s^{-1}}$, to a depth of $150\,\mathrm{m}$) with an eastward component ($\sim 20\,\mathrm{cm\,s^{-1}}$) from $\sim 21°$–$21.5°$W (at $\sim 26°$N) consistent with the ship traversing an anticyclonic structure, north of centre. *In situ* surface chlorophyll-*a* values along the

ship's track (Figure 11) increased in the region near 21°W. SeaSoar sections showed that the *swesty* chlorophyll-*a* signal at 33°W was subsurface with increased levels in the seasonal thermocline ($\sim$100 m depth) where it was domed upwards over the eddy core. Figure 12 shows the seasonal cycle of SeaWiFS chlorophyll-*a* along 25.6°N and the December values are comparable with the *in situ* measurements (cf. Davenport et al., 2002) with elevated levels $(0.3\,\mathrm{mg\,m}^{-3})$ towards the West African Shelf. Since both SeaWiFS chlorophyll-*a* and altimeter structure are annual signals, anomalies in the chlorophyll-*a* seasonal cycle are likely to occur at the same longitude and in the same month each year. This is seen to happen each year near January when the annual westward propagating eddy is on average near 22°W. Developing further, if the coordinates of the structures (position, time) observed in the SeaWiFS cycle are superposed on the altimeter longitude–time plot then it is apparent that they relate to the westward propagating positive anomalies or the *swesty-like propagation*. The simple interpretation is that the eddy core with surface water originating from the east has a more marked spring bloom maximum than the adjacent oceanic water east or west of the eddy (at 25.6°N) and that this signal is carried to the west with the eddy as the bloom decays. However, in addition, or perhaps more probably, the clockwise swirl currents of the eddy have picked up the increased surface chlorophyll-*a* levels to the east and south and that these elevated levels are then carried to the west with the eddy or just ahead of the eddy centre.

REFERENCES

Armi, L. & Stommel, H., 1983. Four views of a portion of the North Atlantic Subtropical Gyre. *Journal of Physical Oceanography*, **13**, 828–857.

Baldacci, A., Corsini, G., Grasso, R., Manzella, G., Allen, J.T., Cipollini, P., Guymer, T.H. & Snaith, H.M., 2001. A study of the Alboran sea mesoscale system by means of empirical orthogonal function decomposition of satellite data. *Journal of Marine Systems*, **29**, 293–311.

Cipollini, P., Cromwell, D., Challenor, P.G. & Raffaglio, S., 2001. Rossby waves detected in global ocean colour data. *Geophysical Research Letters*, **28**, 323–326.

Cromwell, D. & Smeed, D.A., 1998. Altimetric observations of sea level cycles near the Strait of Bab al Mandab. *International Journal of Remote Sensing*, **19**, 1561–1578.

Davenport, R., Neuer, S., Helmke, P., Perez-Marrero, J. & Llinas, O., 2002. Primary productivity in the northern Canary Islands region as inferred from SeaWiFS imagery. *Deep-Sea Research II*, **49**, 3481–3496.

Efthymiadis, D., Hernandez, F. & Le Traon, P.-Y., 2002. Large-scale sea-level variation and associated atmospheric forcing in the sub-tropical north-east Atlantic Ocean. *Deep-Sea Research II*, **49**, 3957–3981.

Fuglister, F.C., 1960. The Atlantic Ocean Atlas of temperature and salinity profiles and data from the International Geophysical Year of 1957–1958. *Woods Hole Oceanographic Institution Atlas Series*, **1**, 1–209.

Germain, C., Tyler, P. & Griffiths, G., 2003. The maiden Voyage of UK ROV Isis. *Ocean Challenge*, **12**, 16–18.

Lavin, A.M., Bryden, H.L. & Parrilla, G., 2003. Mechanism of heat, freshwater and nutrient transports and budgets at 24.5°N in the subtropical North Atlantic. *Deep-Sea Research I*, **50**, 1099–1128.

Le Traon, P.-Y., Nadal, F. & Ducet, N., 1998. An improved mapping method of multi-satellite altimeter data. *Journal of Atmospheric and Oceanic Technology*, **15**, 522–534.

Ledwell, J.R., Watson, A.J. & Law, C.S., 1993. Evidence for slow mixing across the pycnocline from an open-ocean tracer-release experiment. *Nature, London*, **364**, 701–703.

Mouriño, B., Fernández, F., Escánez, J., Armas, D., Giraud, S., Sinha, B. & Pingree, R.D., 2002. A SubTropical Oceanic Ring of Magnitude (STORM) in the Eastern North Atlantic: physical chemical and biological properties. *Deep-Sea Research II*, **49**, 4003–4021.

Ocean Circulation, 2001. Second edition. Butterworth Heinemann Publishers.

Ocean Zone, 2003. Issue 9. Southampton: Southampton Oceanography Centre.

Pingree, R.D., 1996. A shallow subtropical subducting westward propagating eddy (**swesty**). *Philosophical Transactions of the Royal Society* A, **354**, 979–1026.

Pingree, R.D., 1997. The eastern Subtropical Gyre (North Atlantic): flow rings recirculations structure and subduction. *Journal of the Marine Biological Association of the United Kingdom*, **77**, 573–624.

Pingree, R.D., 2002. Ocean structure and climate (Eastern North Atlantic): *in situ* measurement and remote sensing (altimeter). *Journal of the Marine Biological Association of the United Kingdom*, **82**, 681–707.

Pingree, R.D., Kuo, Y.-H. & Garcia-Soto, C., 2002. Can the Subtropical North Atlantic Ocean permanent thermocline be observed from space? *Journal of the Marine Biological Association of the United Kingdom*, **82**, 709–728.

Pingree, R.D. & Sinha, B., 2001. Westward moving waves or eddies (*Storms*) on the Subtropical/Azores Front near 32.5°N? Interpretation of the Eulerian currents and temperature records at moorings 155 (35.5°W) and 156 (34.4°W). *Journal of Marine Systems*, **29**, 239–276.

Pingree, R.D., Sinha, B. & Griffiths, C.R., 1999. Seasonality of the European slope current (Goban Spur) and ocean margin exchange. *Continental Shelf Research*, **19**, 929–975.

PML, 1994. *RRS Charles Darwin Cruise 83/94 Report, 13 December 1993–13 January 1994*. Plymouth: Plymouth Marine Laboratory.

Rapidmoc, 2004. Gulf Stream probed for early warnings of system failure. *Nature, London*, **427**, 769.

Richards, P., 2002. *Westward propagating disturbances at 26°N in the Subtropical North Atlantic using altimeter remote sensing data from ERS1/2 and TOPEX POSEIDON satellites*. Plymouth: Department of Mathematics and Statistics, University of Plymouth.

Roemmich, D. & Wunsch, C., 1985. Two transatlantic sections: meridional circulation and heat flux in the subtropical North Atlantic Ocean. *Deep-Sea Research I*, **32**, 619–664.

Tejera, A., Garcia-Weil, L., Heywood, K.J. & Canton-Garbin, M., 2002. Observations of oceanic mesoscale features and variability in the Canary Islands area from ERS.1 altimeter data, satellite infrared imagery and hydrographic measurements. *Journal of Remote Senmsing*, **23**, 4897–4916.

US WOCE, 2001. *2001 US WOCE Implementation Report*, no. 13. College Station, Texas: US WOCE Office.

Wunsch, C., 2004. Gulf Stream safe if wind blows and Earth turns. *Nature, London*, **428**, 601.